J Mater Sci: Mater Electron (2016) 27:11064–11071
DOI 10.1007/s10854-016-5223-9

Effects of film thickness and sputtering power on properties of ITO thin films deposited by RF magnetron sputtering without oxygen

Amalraj Peter Amalathas[1] · **Maan M. Alkaisi**[1]

Received: 8 May 2016 / Accepted: 18 June 2016 / Published online: 6 July 2016

Abstract In this work, indium tin oxide (ITO) thin films were grown on a glass substrate without introducing oxygen into the growth environment using RF magnetron sputtering technique. The dependence of surface morphological, optical and electrical properties at different film thicknesses and sputtering RF power were investigated. Results showed that these properties were strongly influenced by the film thickness and sputtering RF power. It was found that the resistivity, sheet resistance and optical transmittance of ITO thin films deposited on glass substrate decreased as film thickness increased from 75 to 225 nm while the surface roughness and optical bandgap increased. The optimum properties were obtained for ITO films 225 nm thick grown at 250 W RF power. This has revealed an excellent figure of merit of ($38.4 \times 10^{-4}\ \Omega^{-1}$) with average transmittance (83.3 %), resistivity ($9.4 \times 10^{-4}\ \Omega$ cm), and carrier concentration ($6.1 \times 10^{20}\ \text{cm}^{-3}$). These ITO films are suitable for use in solar cells applications.

✉ Amalraj Peter Amalathas
amalraj.peteramalathas@pg.canterbury.ac.nz

Maan M. Alkaisi
maan.alkaisi@canterbury.ac.nz

[1] Department of Electrical and Computer Engineering, MacDiarmid Institute for Advanced Materials and Nanotechnology, University of Canterbury, Private Bag 4800, Christchurch 8140, New Zealand

1 Introduction

Indium tin oxide (ITO) thin films have been widely utilized in transparent and flexible optoelectronics device fabrication technologies such as liquid crystal displays, plasma display panels, gas sensor, flat panel displays, solar cells and organic light-emitting diodes [1–4]. This is due to their low electrical resistivity and high optical transmission in the visible range. Various coating techniques have been utilized to deposit ITO thin films such as DC/RF magnetron sputtering [5], reactive thermal evaporation [6], ion beam sputtering [7], pulsed laser deposition [8], chemical vapour deposition [9] and spray pyrolysis [10]. Among these techniques, RF magnetron sputtering is one of the most extensively used deposition technique in many industries, due to its inherent advantages such as good reproducibility, low temperature process and large area film deposition capability [11]. However, the properties of ITO film are critically dependent on various deposition parameters, such as working gas pressure, RF power, chamber environment, film thickness, target to substrate distance, substrate temperature, target specification and post deposition treatment [12, 13]. In the majority of reports, oxygen was used as a reactive gas during deposition and/or post-deposition annealing to decrease the resistivity of the films [14–16].

In this study, ITO thin films were grown by RF magnetron sputtering at room temperature without introducing oxygen into the growth environment. The main objective of this study is to evaluate the effects of film thickness and sputtering RF power on the surface morphological, optical and electrical properties of ITO thin films without introducing oxygen into deposition atmosphere. In addition, optimization of film thickness and sputtering RF power without added oxygen to produce high performance ITO suitable for solar cells applications has been demonstrated.

2 Experimental details

2.1 Preparation of ITO thin film

In this work, ITO thin films were deposited on 0.5 mm thick soda-lime glass substrates (20 mm × 20 mm) by RF magnetron sputtering system (Edwards Auto500) using a solid ITO target (90:10 wt% In_2O_3:SnO_2) with a purity of 99.99 %, a diameter of 75 and 5 mm thick. The substrates cleaning procedure were normally carried out by dipping for few minutes in acetone, methanol, and isopropyl alcohol (IPA) solvents in an ultrasonic bath and rinsed with deionized water and then blown dry with Nitrogen gas. The surface was further treated using oxygen plasma for 20 min before being loaded into the sputtering system. The sputterer chamber was pumped down using a turbomolecular pump before introducing the sputtering Ar gas, which had high purity (99.999 %) and free of oxygen. The base pressure of the chamber was in the range of about 3×10^{-6} mbar. The deposition process was carried out in an Ar flow rate of 10 sccm at room temperature (295 K) with a processing pressure of 3.2×10^{-3} mbar. No oxygen was added during the deposition. The substrate holder was continuously rotated during the sputtering to enhance the film's uniformity. The ITO films were grown at different thicknesses ranging from 75 to 225 nm with a 50 nm increment at an RF power of 100 W. The films were also deposited at different RF powers from 100 to 250 W in a 50 W step to produce a fixed thickness of 225 nm. After deposition, the deposited films were diced into 5 mm^2 samples using the Tempress 602 dice saw system for structural, optical and electrical analyses.

2.2 Film characterization

The thickness of the films was measured using a Surface Profilometer DEKTAK 150. The surface morphology of the deposited films was observed by atomic force microscopy (AFM) under ambient air conditions. The optical transmittance spectra of films were carried out by a Cary Spectrophotometer 619 in the wavelength range from 200 to 800 nm. Hall mobility, carrier concentration, and resistivity were measured using Van der Pauw Hall effect measurement method under a magnetic field of 0.51 T. All measurements were conducted at room temperature (295 K).

3 Results and discussion

3.1 Surface morphological analysis

Figure 1a–d shows the AFM images of the surface morphologies of ITO films with thickness ranging from 75 to 225 nm prepared at an RF power of 100 W respectively. Root mean square roughness, Rq, was determined from AFM data of 1 μm × 1 μm scan area. The surface roughness increases slowly as the film thickness increases from 75 to 225 nm. It can be clearly seen from Fig. 2 that, as the thickness reaches 225 nm, the RMS roughness rises up to 12.5 Å. These significant changes in roughness with increasing film thickness is due to the reflecting nucleation, coalescence and continuous film growth processes (Volmer–Weber type) [17]. Figure 1 demonstrates that the RMS value of the roughness is strongly influenced by the degree of aggregation and cluster size of the thin films. This is in agreement with the principle that different cluster or grain size affects the surface roughness of the thin films [18].

Figure 3a–d shows the AFM images of the surface morphologies of the 225 nm thick ITO films prepared with different RF powers in the range from 100 to 250 W. The values of the RMS roughness for the 225 nm thick ITO films deposited with RF power varying from 100 to 250 W are shown in Fig. 4. It is observed that the sputtering RF power also has an influence on the surface structure of ITO films. The ITO films grown at 100 W RF power have the comparatively low kinetic energy of sputtered particles compared to 250 W RF power, which leads to relatively more random orientation and various sizes of grain growth which lead to manifest as a rough surface. The sputtered particles have sufficient energy for uniform distribution of grain growth and thus lead to a smoother surface with increasing in RF sputtering power.

3.2 Electrical properties

Figure 5 illustrates the variation of resistivity, carrier concentration, and Hall mobility of the ITO films grown at an RF power of 100 W as a function of film thickness. Carrier concentration increases rapidly with the film thickness increasing from 75 to 225 nm and reaching a maximum of 1.12×10^{21} cm^{-3}. It is also observed that resistivity decreases with an increase in the film thickness from 75 to 175 nm and remains almost constant afterwards.

Figure 6 shows the sheet resistance and the resistivity as a function of the film thickness. It is found that the sheet resistance decreases rapidly as the ITO film thickness increases from 75 to 125 nm. For further increase of the ITO film thickness, the sheet resistance decreases slowly and the minimum sheet resistance obtained is about 27.5 Ω/sq for a film thickness of 225 nm. The decrease in sheet resistance with increasing film thickness is due to an increase in carrier concentration of the films which results from the enlarged grain size. It has been reported by Kim et al. [19] that grain size increased with an increase in ITO film thickness. The values of the carrier mobility drop with

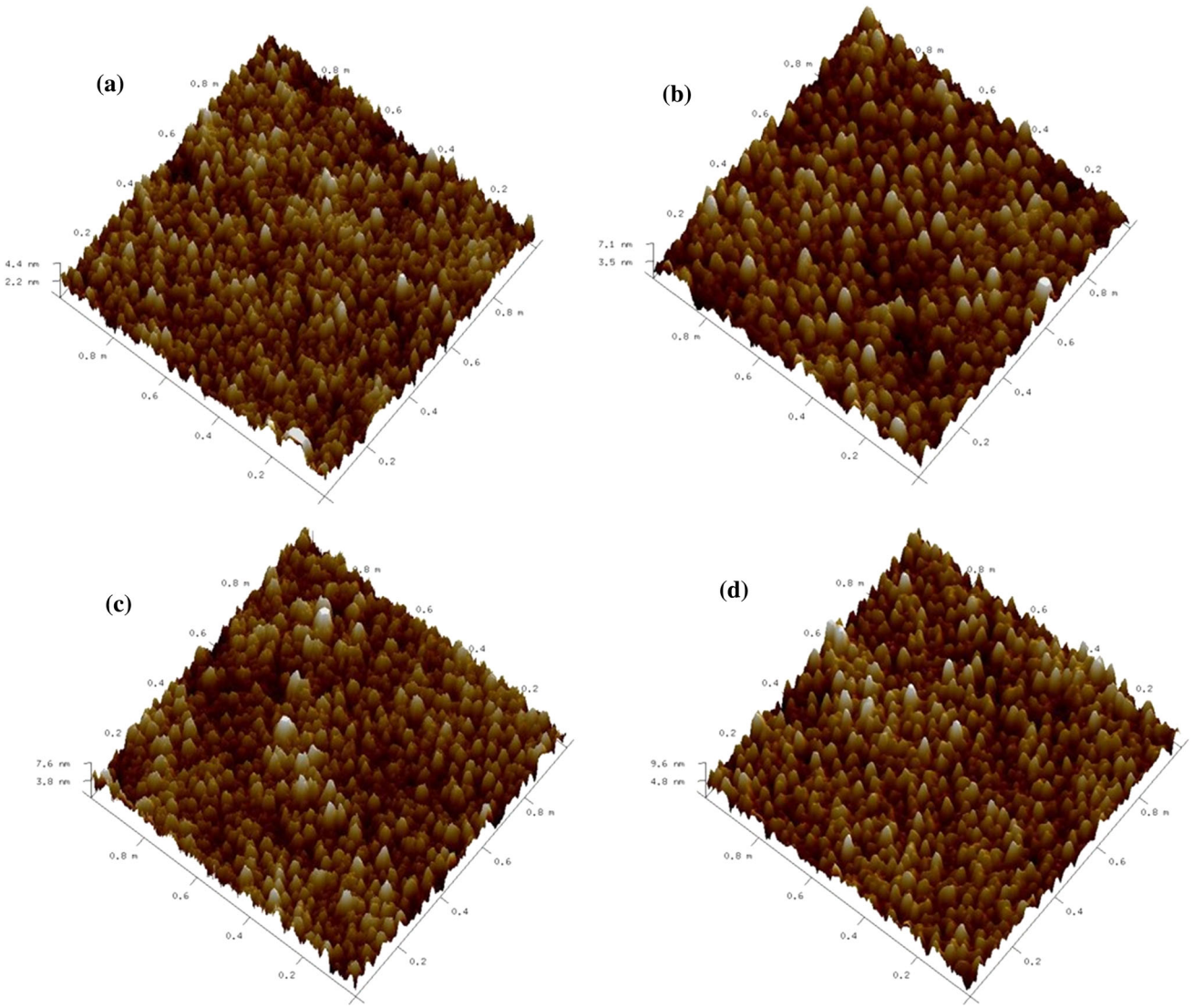

Fig. 1 AFM images of ITO films at an RF power of 100 W with different thicknesses **a** 75 nm, **b** 125 nm, **c** 175 nm, and **d** 225 nm

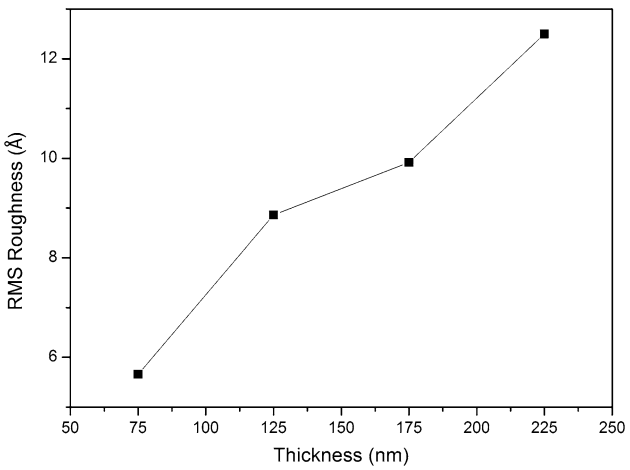

Fig. 2 RMS roughness R_q of the surface of ITO films deposited at an RF power of 100 W with different thicknesses

increased surface roughness, probably, due to the electron scattering at grain boundaries. It has also been reported that the carrier mobility is limited by the grain boundaries [20]. However, the carrier mobility increases as the film thickness increased from 75 to 125 nm then decreases as the film thickness increased from 125 to 225 nm.

Figure 7 shows the electrical resistivity, carrier concentration and Hall mobility of the 225 nm thick ITO films as a function of the RF power. Carrier concentration decreases from 1.12×10^{21} to 6.07×10^{20} cm^{-3} when RF power is increased from 100 to 250 W. This indicates that the damage by negative ion collision influences the carrier concentration. The mechanism of carrier concentration drop by negative ion damage can be explained by the decrease in oxygen vacancies as donors and the increase in bivalent In or Sn as acceptors [21].

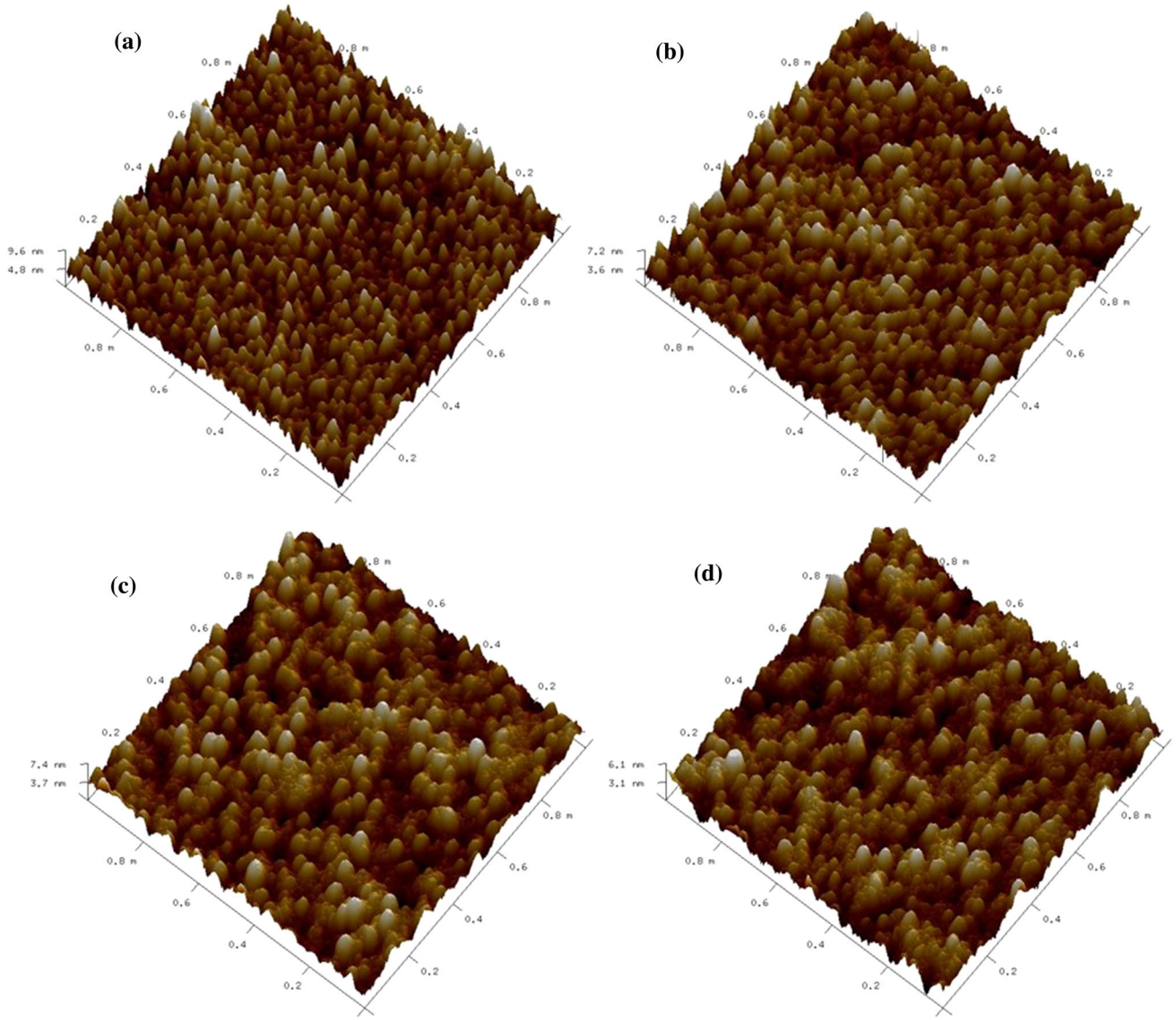

Fig. 3 AFM images of 225 nm thick ITO films with different RF power **a** 100 W, **b** 150 W, **c** 200 W, and **d** 250 W

The carrier mobility increases gradually with RF power in the range from 100 to 200 W then decreases rapidly when the RF power is increased above 200 W. There is a slight fall in the resistivity and sheet resistance for an RF power between 100 and 150 W as shown in the Fig. 8. However, the values of the resistivity increase gradually when the RF power is in the range from 150 to 250 W. The decrease in sheet resistance with an increase in RF power from 100 to 150 W is attributed by a lower collision of negative ions [21]. While for an RF power over 150 W, bombardments became stronger which lead to a low density of Oxygen vacancies. In general, this result indicates that a lower sputtering RF power is preferred for decreasing the resistivity of ITO film.

3.3 Optical properties

Figure 9 shows the optical transmittance spectra of ITO films measured at different thicknesses in the wavelength range of 300–800 nm. Samples were prepared at an RF power of 100 W. The average transmittance of all samples in the visible range is over 75 % as shown in the inset of Fig. 9.

With increasing the thickness from 75 to 225 nm, the average transmittance in the wavelength range of 400–800 nm decreased slowly. This decrease in transmission may be due to free carrier absorption that increases the carrier density in the thicker films. Furthermore, all of the ITO films exhibit sharp absorption edge in the ultraviolet

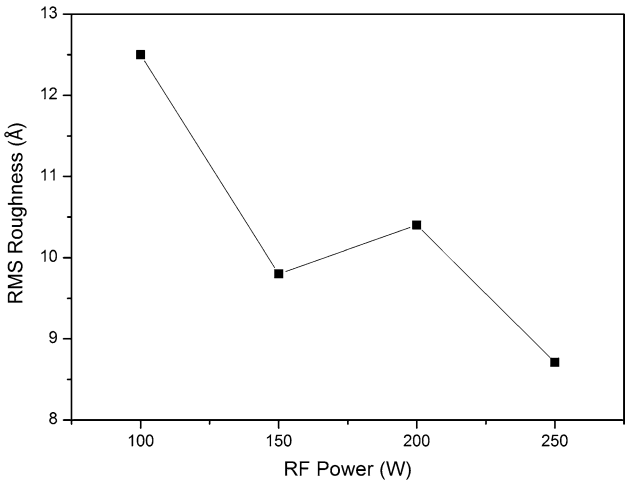

Fig. 4 RMS roughness R_q of the surface of 225 nm thick ITO films deposited with different RF power

region, which may be associated with the direct transition of electrons between the conduction band and valence band. It is seen that the absorption edge shifts gradually to lower photon energy with an increase in the film thickness. It can also be seen that the transmittance in the visible region is influenced by the ITO film structure and surface morphology. As the surface roughness increases with an increase in film thickness, there is a slight enhancement in surface scattering which results in a gradual drop in optical transmittance in the visible region.

The optical absorption coefficient (α) can be estimated using the following formula.

$$\alpha = \frac{\ln(1/T)}{t} \tag{1}$$

where T is the transmittance and t is the thickness of the film.

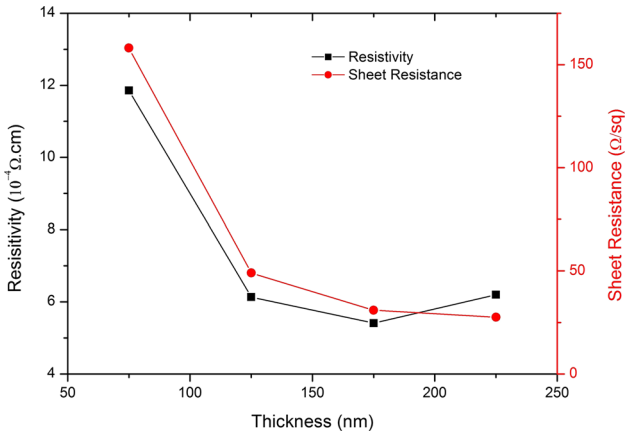

Fig. 6 Variation of the resistivity and sheet resistance of ITO films with film thickness

For a direct band semiconductor of allowed band to band transition, the optical energy band gap (E_g) of the thin films can be calculated by using the value of α in the following equation.

$$\alpha(h\upsilon) = A\left(h\upsilon - E_g\right)^{1/2} \tag{2}$$

where h is Planck's constant, υ is the frequency of the incident photon and A is constant. The optical energy band gap of the film is determined by plotting $(\alpha h\upsilon)^2$ as a function of photon energy ($h\upsilon$), and extrapolating linear portions of $(\alpha h\upsilon)^2$ against photon energy ($h\upsilon$) where $(\alpha h\upsilon)^2$ is zero, then the photon energy is equal to the optical energy band gap.

Figure 10 illustrates the plots of $(\alpha h\upsilon)^2$ against photon energy (hυ) with various film thicknesses at an RF power of 100 W. The inset in Fig. 10 shows the dependence of optical energy band gap, E_g, on film thickness, and the value increases from 3.831 eV for 75 nm sample to

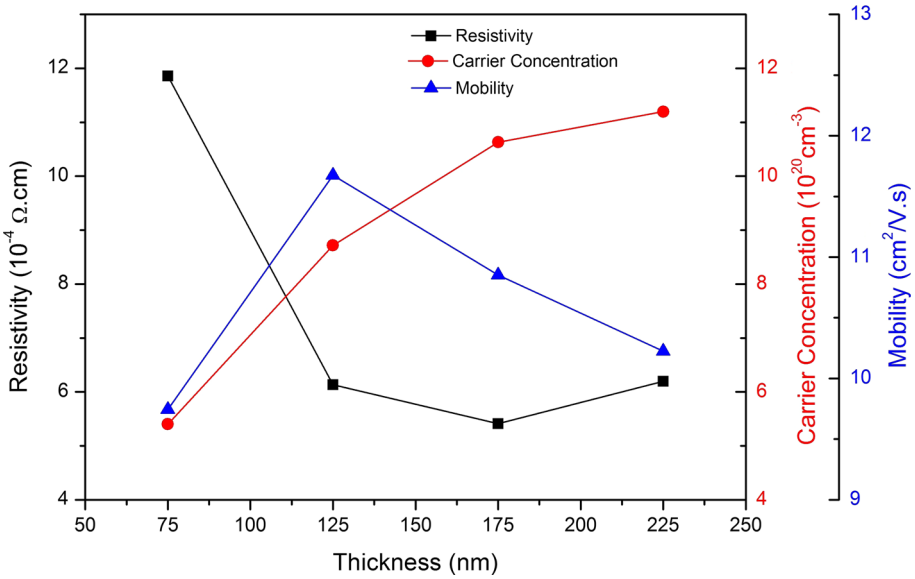

Fig. 5 Variation of the resistivity, carrier concentration and Hall mobility of ITO films with film thickness

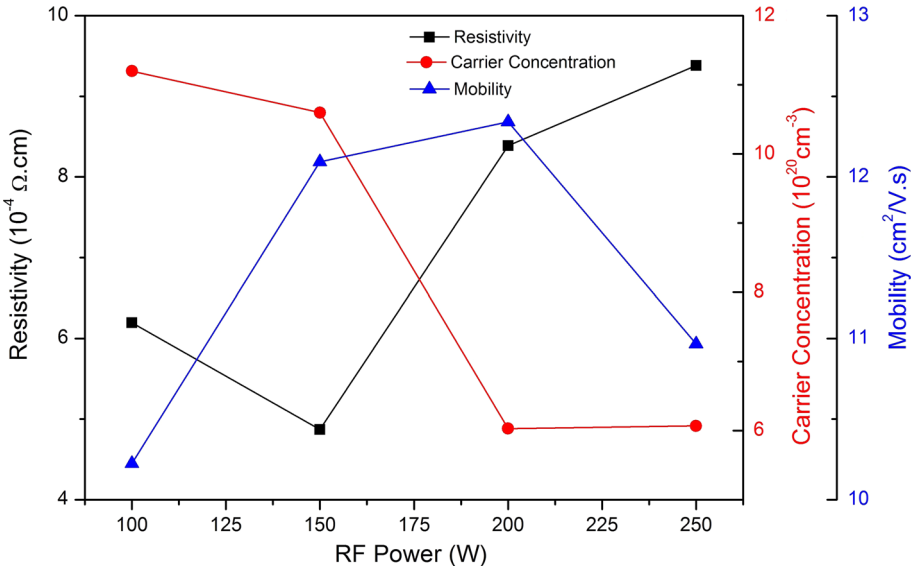

Fig. 7 Variation of the resistivity, carrier concentration and Hall mobility of 225 nm thick ITO films grown at various RF power

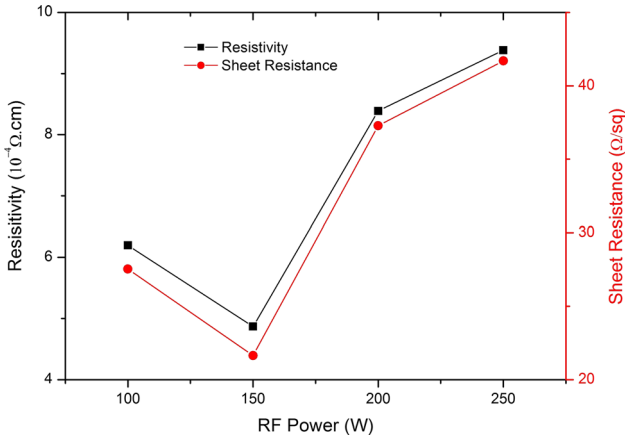

Fig. 8 Variation of the resistivity and sheet resistance of 225 nm thick ITO films grown at various RF power

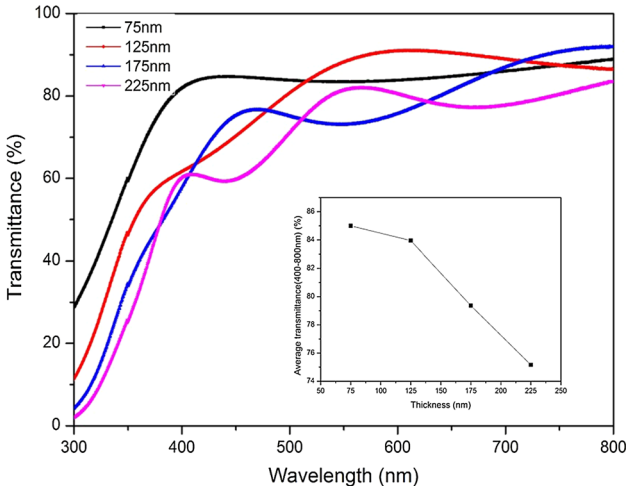

Fig. 9 Optical transmittance of ITO film as a function of wavelength with different thicknesses at RF power of 100 W. *Inset* shows the average transmittance of those ITO film in the wavelength ranges from 400 to 800 nm

4.003 eV for the 225 nm sample. The fact that the increase in optical band gap is correlated to increase in carrier concentration with respect to increased film thickness could also be seen in Fig. 5. This shift of the band gap can be explained by Burstein–Moss shift [22, 23]. Increasing the number of carriers with an increase in film thickness leads to increase in the Fermi level above the bottom of the conduction band, thereby causing an enlargement in the optical band gap of the ITO films.

The optical transmittance spectra of the 225 nm ITO film prepared with different RF power are shown in Fig. 11 in the wavelength range of 300–800 nm. The average transmittance of all samples during the visible range is over 75 %. With increasing RF power, the average transmittance in the wavelength range of 400–800 nm increases gradually from 75.2 % for 100 W sample to 83.3 % for 250 W sample.

Figure 12 illustrates the plots of $(\alpha h\upsilon)^2$ against photon energy ($h\upsilon$) for the 225 nm thick ITO film with various RF powers. The inset in Fig. 12 shows the variations of the optical energy band gap E_g as a function of RF power. The absorption edge shifts towards the higher energy as shown in the Fig. 11 and the energy gap drops from 4.003 to 3.881 eV upon increasing the RF power from 100 to 250 W. These optical energy band gap values have a strong correlation with carrier concentration, which influences the optical band gap.

For the photovoltaic applications, ITO thin films must have low resistivity and high optical transmittance. To obtain the best performance of transparent conducting

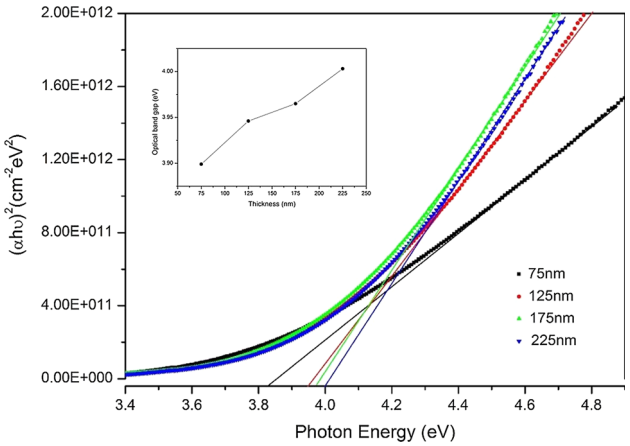

Fig. 10 $(\alpha h\upsilon)^2$ against photon energy ($h\upsilon$) with different film thicknesses at RF power of 100 W. *Inset* shows variation of optical band gap E_g of those ITO films

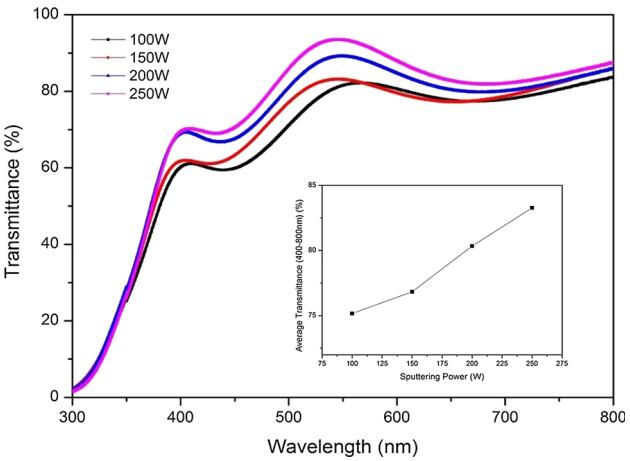

Fig. 11 Optical transmittance of 225 nm thick ITO film as a function of wavelength with various RF power. The *inset* shows the average transmittance of those ITO film in the wavelength ranges from 400 to 800 nm

films, the figure of merit ϕ_{TC}, proposed by Haacke [24], is given by

$$\phi_{TC} = T^{10}/R_S \quad (3)$$

where, T is the average optical transmittance and R_S is the sheet resistance of the films. The values of ϕ_{TC} for the ITO films with different thicknesses and RF sputtering powers are listed in Table 1.

It can be seen that due to its high resistance, the 75 nm thick ITO film prepared at 100 W RF power has a minimum ϕ_{TC} value. The highest value of ϕ_{TC} for films prepared at 100 W was obtained at a thickness of 125 nm. The overall optimum value of figure of merit ϕ_{TC} is $38.4 \times 10^{-4}\ \Omega^{-1}$, this value was obtained for ITO film with thickness of 225 nm and RF power of 250 W. This

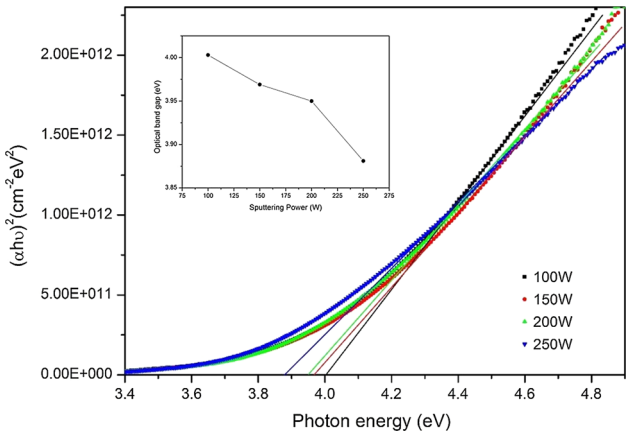

Fig. 12 $(\alpha h\upsilon)^2$ against photon energy ($h\upsilon$) of 225 nm thick ITO film various RF power of 100 W. *Inset* shows variation of optical band gap E_g of those ITO films

Table 1 The thickness and RF sputtering power dependence of figure of merit values of ITO thin films

RF Power (W)	Thickness (nm)	Average transmittance between 400 and 800 nm (%)	Sheet resistance (Ω/sq)	Figure of merit (ϕ_{TC}) ($\times 10^{-4}$ Ω^{-1})
100	75	85.0	158.1	12.4
100	125	84.0	49.1	35.5
100	175	79.4	30.9	32.1
100	225	75.2	27.5	20.9
150	225	76.8	21.6	33.1
200	225	80.3	37.3	30.1
250	225	83.3	41.7	38.4

ITO film fulfills the optical and electrical requirements for efficient photovoltaic applications.

4 Conclusions

In this work, the surface morphological, optical and electrical properties of ITO thin films prepared by RF magnetron sputtering were studied. The films were prepared without introducing oxygen into the growth environment and deposited at different film thicknesses and RF powers at room temperature. This study reveals that both the electrical and optical properties are dependent on film thickness as well as sputtering RF power. AFM images of the ITO thin films reveal that surface roughness value increase with increasing the film thickness from 75 to 225 nm. The grown ITO films exhibit low resistivity and high optical transmission in the visible region. The lowest sheet resistance of the ITO thin films obtained is 21.6 Ω/sq for 225 nm thickness deposited at 150 W RF power. The

average optical transmittance (400–800 nm), carrier concentration, carrier mobility are 76.8 %, 10.6×10^{20} cm^{-3}, and 12.1 cm^2/V.s, respectively. For the photovoltaic applications, both excellent optical transmittance and high conductivity are required. The 225 m thickness ITO films prepared at 250 W RF power have a suitable figure of merits values, which exhibits 83.3 % average optical transmittance (400–800 nm), 9.4×10^{-4} Ω cm resistivity, 6.1×10^{20} cm^{-3} carrier concentration and an 11 cm^2/V.s carrier mobility. These films are suitable for photovoltaic device applications especially organic, and thin films solar cells.

Acknowledgments The authors would like to thank Gary Turner and Helen Devereux from the Nanofabrication Laboratory, University of Canterbury, New Zealand for providing technical assistance and Prof. Roger Reeves for transmittance measurements. Amalraj PA acknowledges the UC Doctorate Scholarship, University of Canterbury, New Zealand.

References

1. H. Kim, A. Pique, J. Horwitz, H. Mattoussi, H. Murata, Z. Kafafi, D. Chrisey, Appl. Phys. Lett. **74**, 3444 (1999)
2. G. Li, C.-W. Chu, V. Shrotriya, J. Huang, Y. Yang, Appl. Phys. Lett. **88**, 253503 (2006)
3. N. Patel, P. Patel, V. Vaishnav, Sens. Actuator B-Chem. **96**, 180 (2003)
4. H. Liu, V. Avrutin, N. Izyumskaya, Ü. Özgür, H. Morkoç, Superlattices Microstruct. **48**, 458 (2010)
5. S. Najwa, A. Shuhaimi, N. Ameera, K. Hakim, M. Sobri, M. Mazwan, M. Mamat, Y. Yusnizam, V. Ganesh, M. Rusop, Superlattices Microstruct. **72**, 140 (2014)
6. A. Amaral, P. Brogueira, C.N. De Carvalho, G. Lavareda, Surf. Coat. Technol. **125**, 151 (2000)
7. D. Kim, Y. Han, J.-S. Cho, S.-K. Koh, Thin Solid Films **377**, 81 (2000)
8. J.H. Kim, K.A. Jeon, G.H. Kim, S.Y. Lee, Appl. Surf. Sci. **252**, 4834 (2006)
9. T. Maruyama, K. Fukui, Thin Solid Films **203**, 297 (1991)
10. S. Rozati, T. Ganj, Renew. Energy **29**, 1671 (2004)
11. K. Ellmer, T. Welzel, J. Mater. Res. **27**, 765 (2012)
12. H. Park, S. Q. Hussain, S. Velumani, A.H.T. Le, S. Ahn, S. Kim, J. Yi, Mat. Sci. Semicond. Proc. **37**, 29 (2015)
13. D. Song, Appl. Surf. Sci. **254**, 4171 (2008)
14. Y.J. Kim, S.B. Jin, S.I. Kim, Y.S. Choi, I.S. Choi, J.G. Han, Thin Solid Films **518**, 6241 (2010)
15. H.-C. Lee, O.O. Park, Vacuum **75**, 275 (2004)
16. F. Adurodija, H. Izumi, T. Ishihara, H. Yoshioka, M. Motoyama, K. Murai, J. Vac. Sci. Technol. A **18**, 814 (2000)
17. Y. Shigesato, R. Koshi-Ishi, T. Kawashima, J. Ohsako, Vacuum **59**, 614 (2000)
18. R. Buzio, E. Gnecco, C. Boragno, U. Valbusa, P. Piseri, E. Barborini, P. Milani, Surf. Sci. **444**, L1 (2000)
19. H. Kim, J. Horwitz, G. Kushto, A. Pique, Z. Kafafi, C. Gilmore, D. Chrisey, J. Appl. Phys. **88**, 6021 (2000)
20. H.R. Fallah, M. Ghasemi, A. Hassanzadeh, H. Steki, Phys. B **373**, 274 (2006)
21. S. Ishibashi, Y. Higuchi, Y. Ota, K. Nakamura, J. Vac. Sci. Technol. A **8**, 1403 (1990)
22. E. Burstein, Phys. Rev. **93**, 632 (1954)
23. T. Moss, Proc. Phys. Soc. Sect. B **67**, 775 (1954)
24. G. Haacke, J. Appl. Phys. **47**, 4086 (1976)